PCCP

ROYAL SOCIETY OF CHEMISTRY

PAPER

View Article Online
View Journal | View Issue



Cite this: *Phys. Chem. Chem. Phys.*, 2024, **26**, 24279

# Calcite–aragonite transformation in an eggshell: a crucial role of organics and assessment of the impact of milling conditions on its extent using Taguchi design†

Kairat Kenges,[ab] Stephanos Karafiludis,[c] Róbert Džunda,[d] Imelda Octa Tampubolon,[a] Bagdat Satybaldiyev,[b] Franziska Emmerling[c] and Matej Baláž*[a]

Received 10th June 2024,
Accepted 15th August 2024

DOI: 10.1039/d4cp02354d

rsc.li/pccp



Phase transformations during high-energy ball milling, a tool of mechanochemistry, are interesting due to the possible production of metastable phases without the need for artificially introducing high temperatures and pressures. In our work, the transformation of calcite to aragonite in an eggshell is studied in detail. The presence of organic material, in either the naturally present eggshell membrane, or artificially supplied L-cysteine, was found to be crucial for the phase transformation to occur, its decomposition leading to a pressure increase necessary for aragonite formation. The presence of sulfur in the organics seems to be crucial, as corroborated by much lower phase transformation extent when utilizing sulfur-free organics for comparison. The degree of the transformation in an eggshell was strongly dependent on the used milling conditions. The optimization was assessed using the Taguchi method, namely using a $4^4$ orthogonal array. The optimized parameters encompassed milling time, sample mass, milling speed and duration of breaks and it was shown that sample mass has a decisive effect on the amount of obtained aragonite. Under the most efficient conditions, 73.7% of aragonite was obtained. Prolonging milling until 4 hours further boosts the transformation, reaching 89.9% of aragonite, but further milling leads to the collapse of the aragonite structure and pure calcite was observed after 5 hours.

## 1. Introduction

The possibility of performing phase transformations using high-energy milling has been attracting interest from researchers for a long time[1–6] due to the fact that many high-pressure and/or high-temperature crystal structures (including metastable ones) can be formed even at room temperature and ambient pressure in this way.[7–9] This topic was investigated among pioneering works in the field, *e.g.* the transformations in $TiO_2$ (from anatase to srilankite and rutile),[8] $Al_2O_3$ (from the γ- to the α-phase),[10] and metallic Co (from face-center-cubic to hexagonal close-packed)[11] were described.

Among other phase transformations, the calcite-to-aragonite one is of particular interest, due to several reasons: on the one hand, changing the structure into aragonite allows the improvement of some properties of the material;[6,12,13] on the other hand, we can find important coincidences with natural phenomena like biomineralization, which develops the knowledge on the management of crystal phases, morphology and architecture using biomimetic processes.[14,15] Most transformations investigated in this system were scrutinized starting from the calcite mineral.[16–20] The process was usually very time-consuming[21,22] and the question "What is behind this transformation?" remained unanswered for a long time.

Apart from the mineral, calcite is also present in the eggshell waste. The eggshell (ES) is a waste material exhaustively studied for its potential applications in materials science due to its unique properties.[23] The primary component of ES is calcium carbonate (~95%) in the form of calcite. Apart from that, proteins (an organic matrix corresponding to 3.3–3.5% and

[a] *Institute of Geotechnics, Slovak Academy of Sciences, Watsonova 45, 04001 Košice, Slovakia. E-mail: kenges.qayrat@gmail.com, balazm@saske.sk*
[b] *Center of Physical–Chemical Methods of Research and Analysis, Al-Farabi Kazakh National University, Tole bi 96A, 050012 Almaty, Kazakhstan. E-mail: bagdat.satybaldiev@gmail.com*
[c] *Federal Research Institute for Materials Testing, Richard-Wiltstätter Strasse 11, 12489 Berlin, Germany. E-mail: stefanos.karafiludis@bam.de, franziska.emmerling@bam.de*
[d] *Institute of Materials Research, Slovak Academy of Sciences, Watsonova 47, 04001 Košice, Slovakia. E-mail: rdzunda@saske.sk*

† Electronic supplementary information (ESI) available. See DOI: https://doi.org/10.1039/d4cp02354d

1.6% water of the shell weight) that interact with the mineral phase controlling its formation and structural organization during eggshell development are also present,[24,25] and thus determine the mechanical properties of the mature biomaterial. These proteins form the fibrous eggshell membrane that separates the eggshell from the inner part of the egg and is also interesting for particular applications in materials science.[26]

It was possible to transform calcite to aragonite in the eggshell quite rapidly by exerting enough energy.[5,13,27] If enough energy is not supplied, the transformation will not occur.[28] The presence of the organic membrane seemed to speed up the process,[13] but whether its presence is mandatory for the transformation to occur and the possibility of its replacement by an artificially introduced organic material was not investigated.

The aim of the present study was exactly to provide an answer to these questions. A key role of the presence of the eggshell membrane to trigger the transformation, and also a possibility to induce it by the presence of an artificially introduced organic material, was revealed. Moreover, the effect of the individual milling parameters on the studied phase transformation was assessed using a statistical approach.

# 2. Materials and methods

## 2.1. Materials

Raw eggshells (ES) were obtained from the local canteen. In most cases, the eggshell membrane (ESM) was not separated, and thus this material is referred to as ES + ESM in further text. The eggshells were properly washed with distilled water, dried at laboratory temperature and the powder was crushed to a size below 1 mm using a kitchen mixer. Commercial calcium carbonate (LACHEMA, Czechia) used for comparison and L-cysteine (≥97%, Sigma Aldrich), glycine (≥99%, Sigma Life Science, USA) and polyvinyl pyrrolidone (Sigma Aldrich, USA) used as an artificially introduced organic material were used without further purification.

**2.1.1. Separation of inner and outer eggshell membranes.** For some specific cases, the utilization of ESM-free eggshell was necessary. In this case, a small hole on the top side of a fresh egg was made and then the inner contents were poured out through it. The emptied egg was then washed multiple times with a tap water and left to dry for about 3–6 hours stored upside down so that residual water could leak out through the hole. This time was found to be ideal so that the material was neither too wet nor too dry to remove the eggshell membranes. The eggshell was then vertically broken into two parts in such a way that the air cell present at the bottom part could be preserved in both halves. The inner membrane was then mechanically pulled off from the inside in a soft manner, starting from the air cell. The outer membrane was separated from the eggshell by gently breaking the small fragments of the eggshell and tearing it off from the outer ESM. The ESM-free ES was dried and its particle size was reduced to below 200 μm using a kitchen mixer.

Table 1 The milling conditions for the mechanical activation of eggshell designed according to a Taguchi $4^4$ orthogonal array

| Sample abbreviation | Milling time, h | Sample mass, g | Milling speed, rpm | Break duration, min |
|---|---|---|---|---|
| T1 | 1 | 7 | 400 | 120 |
| T2 | 1 | 5 | 500 | 30 |
| T3 | 1 | 3 | 600 | 15 |
| T4 | 1 | 1 | 700 | 5 |
| T5 | 2 | 7 | 500 | 15 |
| T6 | 2 | 5 | 400 | 5 |
| T7 | 2 | 3 | 700 | 15 |
| T8 | 2 | 1 | 600 | 5 |
| T9 | 3 | 7 | 600 | 120 |
| T10 | 3 | 5 | 700 | 15 |
| T11 | 3 | 3 | 400 | 30 |
| T12 | 3 | 1 | 500 | 120 |
| T13 | 4 | 7 | 700 | 30 |
| T14 | 4 | 5 | 600 | 120 |
| T15 | 4 | 3 | 500 | 5 |
| T16 | 4 | 1 | 400 | 15 |

## 2.2. Methods

**2.2.1. Mechanical activation of the eggshell.** Mechanical activation of the eggshell was carried out in a Pulverisette 7 premium line (P7) laboratory planetary ball mill (Fritsch, Germany) under the following conditions: tungsten carbide milling chamber with a volume of 45 mL, 18 tungsten carbide balls with a diameter of 10 mm and a total weight of 135 g in an air atmosphere. In order to optimise the other milling conditions, design of experiments (DoE), namely the Taguchi method was applied.[29,30] Four factors (milling time, sample mass, milling speed and break duration) were selected and modified at four levels (see Table 1). The initial values were determined based on our previous study.[13] An orthogonal Taguchi array ($4^4$) was created using Minitab14 software (Minitab, Ltd, UK) and sixteen experiments with different combinations were planned.

## 2.3. Characterization techniques

**2.3.1. X-ray diffraction (XRD).** The XRD patterns of the mechanically activated samples were collected using a D8 Advance diffractometer (Bruker, Germany) with Cu$K_\alpha$ radiation in the Bragg–Brentano configuration. The generator was set up at 40 kV and 40 mA. The divergence and receiving slits were set to 0.3° and 0.1 mm, respectively. The XRD patterns were recorded in the range of $2\theta$ = 6–70° with a step of 0.01° and a step time of 3 s. The JCPDS PDF-2 database was utilized for the phase identification. Refinement by using the Le Bail method was performed to obtain phase composition and unit cell parameters using the GSAS-II software package.[31] The precision of phase fraction measurements using the Le Bail refinement method was assessed through the analysis of duplicates, with %RSD being less than 5%. The total uncertainty of refinement by using the Le Bail method was estimated to be 15%, which includes the relative error of diffractometer calibration and the standard deviation of independent phase composition measurements. The prepared synthetic mineral mixtures with different phase compositions of aragonite (PDF 00-041-1475), calcite (PDF 00-066-0867), witherite ($BaCO_3$, PDF 96-100-0034),

 

villiaumite (NaF, PDF 96-900-8680) and strontianite ($SrCO_3$, PDF 96-500-0094) were used; the measured phase composition deviated by less than 10% from the reference values (an example of this assessment is shown in Fig. S1 in the ESI†).

**2.3.2. Scanning electron microscopy (SEM).** The morphology and size of the powder particles were investigated by using a scanning electron microscope (SEM) Tescan Vega 3 LMU (Tescan, Czech Republic) using an accelerating voltage of 20 kV. In order for the samples to be conductive, the powder was covered by a layer of gold using a Fine Coat Ion Sputter JFC 1100. To obtain information about the chemical composition of particles, an energy-dispersive X-ray spectrometer (EDX) with Tescan Bruker XFlash Detector 410 M (Bruker, Germany) was used.

**2.3.3. Specific surface area analysis.** A nitrogen adsorption apparatus NOVA 1200e Surface Area & Pore Size Analyzer (Quantachrome Instruments, United Kingdom) was employed to determine specific surface area ($S_{BET}$). It was calculated using the Brunauer–Emmett–Teller (BET) equation in the region of relative pressures 0.05–0.35.

# 3. Results and discussion

## 3.1. X-ray diffraction and $S_{BET}$ analysis

The effect of different milling conditions on the phase transformation of calcite to aragonite in ES + ESM was investigated by using XRD. The results for the samples T1–T16 are shown in Fig. 1(a and b). The initial material contained only calcite and its XRD pattern is provided in the ESI† (Fig. S2).

The phase transformation clearly proceeds to a different extent (reaching maximum 73.7% for the sample T16) depending on the milling conditions, as aragonite diffraction peaks were observed in the majority of the XRD patterns. The content of aragonite for each sample was assessed through the Le Bail method and the fitting results are presented in Fig. S3 in the ESI.†

According to the literature,[27] the phase transformation of calcite to aragonite in eggshells with the membrane proceeds quite rapidly. Namely, it begins after 15 minutes of milling[22] and the maximum amount of aragonite for eggshell (65%) was

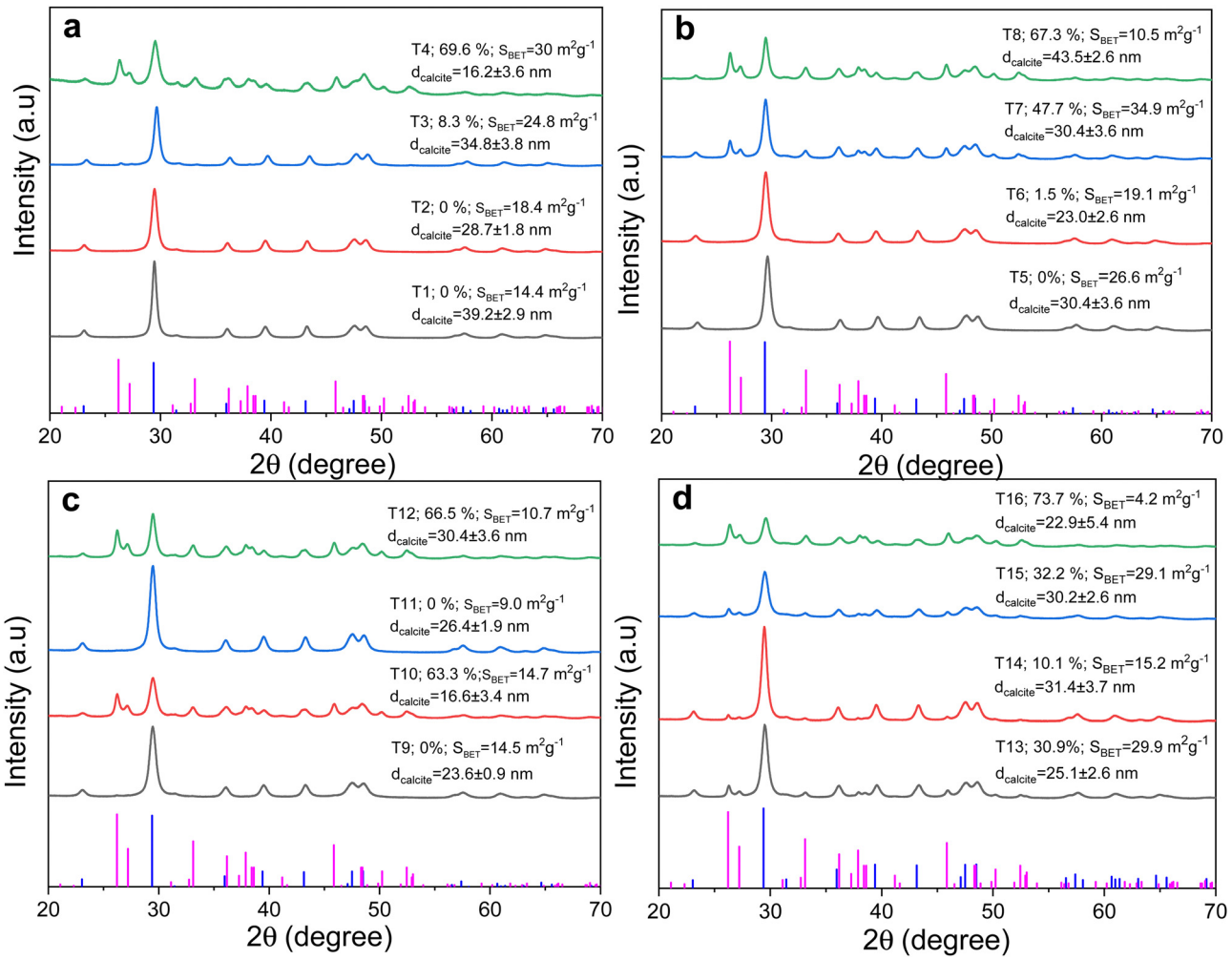


Fig. 1 X-ray diffraction patterns of the ES + ESM treated under T1–T16 conditions: (a) T1–T4, (b) T5–T8, (c) T9–T12, and (d) T13–T16. For comparison, also the initial ES + ESM is included in (a). Blue bars correspond to calcite (00-066-0867) and magenta ones to aragonite (00-041-1475). The percentage content of aragonite calculated by Le Bail refinement is presented in the figure (the rest corresponds to calcite). Also, the crystallite size of calcite (C) and aragonite (A, when present), together with the specific surface area ($S_{BET}$) values for each sample are presented in the figure.

reached after 240 minutes of the treatment. The relatively rapid onset of transformation in eggshell is explained by the porosity and large surface area of the material. This theory is consistent with the results of other works,[13] where eggshell milling was conducted in the absence of the outer eggshell membrane. In the mentioned work, the transformation of calcite to aragonite starts after 30 minutes of milling, and the maximum amount of aragonite (58%) is reached after 360 minutes. However, the potentially important role of the organic eggshell membrane in the phase transformation is not discussed in those studies.

The specific surface area ($S_{BET}$) values for T1–T16 samples are in the range from 9 $m^2\ g^{-1}$ to 34.9 $m^2\ g^{-1}$. The values seem to be independent from aragonite content. The maximum $S_{BET}$ value is observed for sample T7, where the content of aragonite is 47.7%. The maximum $S_{BET}$ value without aragonite content was found for the sample T5 (26.6 $m^2\ g^{-1}$). This is in accordance with ref. 13 where after 30 min maximum surface area (28.4 $m^2\ g^{-1}$) was detected, and the content of aragonite was yet negligible after such a short time.

Using the Le Bail refinement, we have calculated the crystallite size of calcite in all 16 samples. The results are also reported in Fig. 1. The calculated values were between 16 and 43 nm for all the samples, thus nanocrystalline calcite was present in all the samples. The calcite crystallite size in the initial material was 42 ± 5 nm, and thus, already the mildest treatment utilized in experiment T1 led to a significant crystallite size reduction. In comparison with other studies,[17] we do not observe a sharp increase in the size of calcite crystallites, which may be due to the conditions of mechanical activation of calcite. In addition, the formation of the aragonite phase can affect the size of calcite crystallites.[13] For the samples, in which a considerable amount of aragonite was identified, its crystallite size was also determined. The results are in the ESI† in Table S1. Thus, aragonite is also nanocrystalline and its size does not differ significantly from the size of calcite. There is a certain pattern of decreasing dimensions with decreasing sample mass and processing speed. As suggested,[13] more calcite crystals may simultaneously participate in the recrystallization process, and the resulting aragonite is larger in size.

The proposed phase transformation mechanism can be influenced by milling conditions[20,32] and materials properties.

In order to investigate whether there is any relationship between the aragonite content, $S_{BET}$ value and calcite crystallite size, all the combinations of these three properties were plotted against each other (Fig. S4, ESI†). The presented plots revealed that there is no relationship between calcite crystallite size and $S_{BET}$ value and neither does calcite crystallite size seem to depend on the aragonite content. However, when plotting $S_{BET}$ *vs.* the aragonite content, an increase of $S_{BET}$ up to 50% of aragonite and a steep decrease can be observed afterwards. This behavior is correlated with what was observed in the kinetic study in 2015;[13] however, in our case, the decrease is much more pronounced and the $S_{BET}$ values of the most samples with aragonite content higher than 60% are below 15 $m^2\ g^{-1}$.

### 3.2. Taguchi calculations and regression analysis

One of the main advantages of the Taguchi method is to determine the optimum milling conditions without the need to perform the experiments with all the combinations of input parameters.[30] In the present case, our aim was to achieve the highest degree of phase transformation possible, *i.e.* to maximize aragonite yield. Therefore, the-larger-the-better approach was used. The optimum parameters turned out to be milling time 4 hours, sample mass 1 g, milling speed 700 rpm, break duration 15 minutes (Fig. S5, ESI†). However, as the contribution of the milling time and break duration is not very important (this is clear from the low changes in the mean of means in Fig. S5 (ESI†) and will be confirmed later by the ANOVA analysis), we have decided to select the lowest milling time (1 hour) and shortest break (5 minutes) as optimum, in order to save time and energy. We respected the results of Taguchi analysis in the case of the other two parameters, and thus the optimum conditions of T4 experiment were selected.

The Taguchi $3^3$ orthogonal array has been quite recently used for the calcite-to-aragonite phase transformation in a planetary ball mill with the aim of obtaining the lowest crystallite size of calcite.[33] The authors found that milling speed 600 rpm, milling time 10 hours and ball-to-powder ratio 20 were the most suitable. They also succeeded in confirming the predicted value by the reaching a good match with the results of the actual experiment preformed under these conditions. As a starting material, they used commercial calcite powder and stainless steel was used as a material of milling media. Regarding calcite–aragonite phase transformation, the aragonite presence could be clearly distinguished from the XRD patterns only in the sample treated under the most severe conditions, namely under ball-to-powder ratio 50, at 600 rpm for 5 hours.

The data obtained in the present contribution can be used to calculate the individual contribution of each parameter to the outcome *via* Analysis of Variance (ANOVA). The results are summarized in Fig. 2. It can be seen that for aragonite content, the most important factor is sample mass (65%). The confidence level for the calculations was set to 95%, so the *p*-value below 0.05 means that the change of the investigated parameter is statistically significant. As for the sample mass, the *p*-value is equal to 0.005, the statistical significance of this parameter is confirmed. The break duration has the lowest impact on the result (2%). Interestingly, for the calcite crystallite size reduction investigated in ref. 33, sample mass (regarded as ball-to-powder ratio in the mentioned study) was the least important factor out of the three (its contribution being 21%, while that of milling speed and milling time was 32 and 28%, respectively).

The aim of the recent contribution was also to determine the most suitable regression being able to estimate aragonite content. We have tried many regressions available in MINITAB14 software. By utilizing the ''Best subsets'' function, we obtained the information about the regression suitability when

 

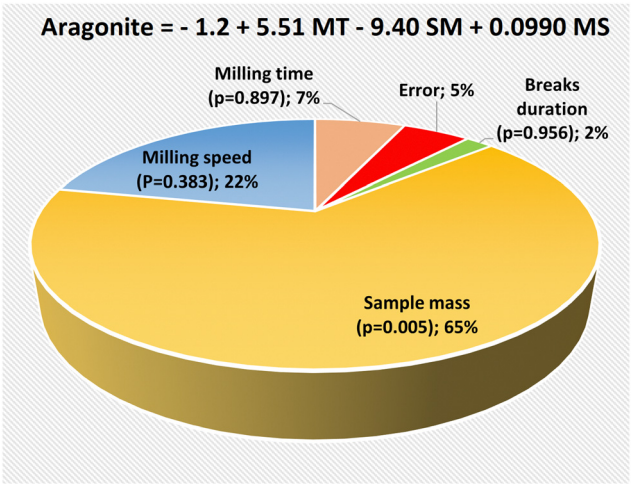


Fig. 2 Analysis of variance (ANOVA) results showing the contributions of individual milling parameters (in %) to the degree of phase transformation in eggshell (aragonite content) and *p* values. The regression is also included: MT – milling time, h; MS – milling speed, rpm; SM – sample mass, g.

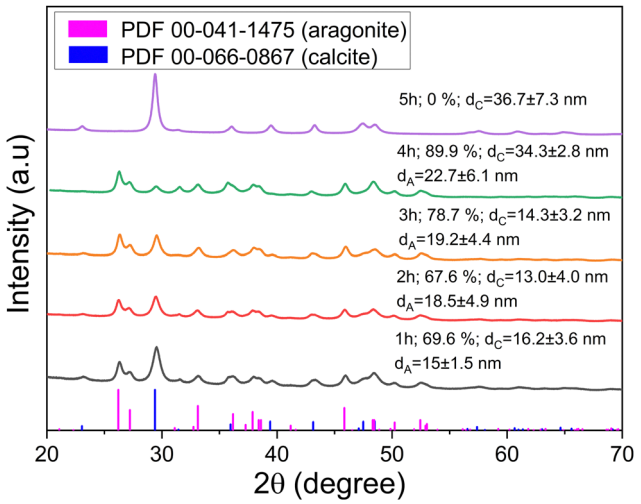


Fig. 3 X-ray diffraction patterns of the ES + ESM after MA using T4 conditions for 1–5 hours. The percentage content of aragonite calculated by Le Bail refinement and the estimated calcite and aragonite crystallite sizes are presented in the figure.

all the combinations of multiple variables are used. The results can be found in Table 2. In addition, by using the ''Fitted line plot'' function, we also investigated the suitability of quadratic and cubic functions of each one of the variables, which is also included in the table.

The regressions for each of the trials are provided in Table S2 in the ESI.† According to the analysis the highest correlation coefficients were obtained when using equation no. 10 possessing three independent variables (break durations are not included). The mentioned equation is given on the top of Fig. 2.

The normality test of the residuals for this equation was performed, which showed that the *p*-value is significantly higher than 0.05, which means that the residuals are normally distributed (Fig. S6, ESI†). This means that the proposed equation quite nicely fits the experimental results.

Table 2 Regression analysis: best subsets and fitted line plots for the regressions available in the MINITAB14 software and corresponding correlation coefficients

| | Variables | | | | | | | | |
|---|---|---|---|---|---|---|---|---|---|
| No. | MT | SM | MS | BD | Equation type | *R*-sq | *R*-sq (adj) | Mallows C-p | S |
| 1 | | x | | | Linear | 51.2 | 47.7 | 5.8 | 21.936 |
| 2 | | | x | | | 14.2 | 8.1 | 19.3 | 29.086 |
| 3 | x | | | | | 4.4 | 0.0 | 22.9 | 30.702 |
| 4 | | | | x | | 0.1 | 0.0 | 24.5 | 31.390 |
| 5 | | x | x | | | 65.4 | 60.1 | 2.6 | 19.170 |
| 6 | x | x | | | | 55.6 | 48.8 | 6.2 | 21.715 |
| 7 | | x | | x | | 51.3 | 43.8 | 7.8 | 22.749 |
| 8 | x | | x | | | 18.6 | 6.1 | 19.7 | 29.401 |
| 9 | | | x | x | | 14.3 | 1.1 | 21.3 | 30.173 |
| 10 | x | x | x | | | 69.8 | 62.2 | 3.0 | 18.643 |
| 11 | | x | x | x | | 65.5 | 56.8 | 4.6 | 19.935 |
| 12 | x | x | | x | | 55.7 | 44.6 | 8.2 | 22.585 |
| 13 | x | | x | x | | 18.7 | 0.0 | 21.7 | 30.590 |
| 14 | x | x | x | x | | 69.8 | 58.9 | 5.0 | 19.452 |
| 15 | x | | | | Quadratic | 4.6 | 0.0 | | 31.826 |
| 16 | | x | | | | 60.7 | 54.7 | | 20.427 |
| 17 | | | x | | | 18.9 | 6.5 | | 29.339 |
| 18 | | | | x | | 0.1 | 0.0 | | 32.562 |
| 19 | x | | | | Cubic | 4.7 | 0.0 | | 33.113 |
| 20 | | x | | | | 64.6 | 55.7 | | 20.191 |
| 21 | | | x | | | 21.7 | 2.1 | | 30.008 |
| 22 | | | | x | | 2.5 | 33.5 | | 33.485 |

*R*-sq: statistical measure in a regression model that determines the proportion of variance in the dependent variable that can be explained by the independent variable, *R*-sq (adj): a modified version of *R*-squared that takes into account the number of predictor variables in the model, Mallows C-p: a statistical measure that compares the performance of a linear regression model to an ideal model that includes all the important predictors, *S* – standard error of the regression. Variables abbreviations: MT – milling time, SM – sample mass, MS – milling speed, BD – breaks duration

### 3.3. Kinetics of the phase transformation under optimum conditions

The phase transformation was already quite pronounced after the treatment under T4 conditions (the content of aragonite was 69.6%). This is much faster than reported at 500 rpm, where such high content of aragonite was not observed even after 6 hours of planetary ball milling. In order to investigate whether the calcite–aragonite transformation can be brought to completion and to have a better overview of the kinetics of the process, we performed milling under T4 conditions for 2, 3, 4 and 5 hours, each time starting with the new batch. The XRD patterns are shown in Fig. 3.

The phase transformation has advanced during the next three hours of treatment; however, it progressed much less rapidly than within the first hour. Namely, only 19.9% calcite was transformed in between 1 and 4 hours of milling. Nevertheless, after four hours, the degree of calcite–aragonite transformation in eggshell is still the largest ever reported (much higher than that in ref. 13). This is most probably due to the presence of both membranes, *i.e.* larger amount of organic material, as will be hypothesized in the next section. However, the complete transformation could not be observed. Upon prolonging the milling to 5 hours, the aragonite crystal structure collapsed and only calcite was identified. The same backward transformation (albeit only to much lower extent) also occurred when treating inner-membrane free eggshell in a planetary ball mill for 16 hours.[5] Similar aragonite-to-calcite transformation seems to also occur when treating commercial calcite powder,[17] judging from the XRD patterns provided therein, albeit the time scales are much longer than in our study. Although we are unable to explain this quick backward transformation at the moment, the hypothetical explanation could be that once all the organics necessary for the transformation are decomposed, the metastable aragonite is quickly transformed back into calcite due to the absence of the heat and pressure created during organics decomposition necessary for maintaining aragonite polymorph during further milling. The aragonite crystallite size is gradually increasing with milling time (from 15 nm after 1 hour to 23 nm after 4 hours). On the other hand, the estimated crystallite size of calcite remains almost the same (around 15 nm) until 3 hours and then significantly increases to 34 nm after 4 hours. This increase might be related to the approaching termination of aragonite formation. After aragonite disappearance, the crystallite size of calcite was only barely affected.

A complete calcite–aragonite transformation might potentially be achieved by artificially adding more organic material, which creates a great playground for the future research. In general, the best solution to get real-time information about the phase transformation would be performing time-resolved *in situ* X-ray diffraction monitoring,[34,35] so an effort in this direction will be made in the future.

### 3.4. Influence of membrane presence

All the results mentioned so far were obtained for the ES containing ESM. It was shown in the past that the presence of ESM enhances the rate of the phase transformation of $CaCO_3$ in eggshell.[13] The material labelled as ES in the mentioned study still contained outer membrane, as although the ESM is reported to be separated by boiling in a weak solution of hydrochloric acid, this process only separates the inner membrane, while the outer membrane remains firmly bound to the ES (we discovered this when closely analyzing the eggshells after boiling). Nevertheless, a small difference in favor of the progress of the calcite–aragonite transformation in the material containing both membranes can be clearly seen in that study.

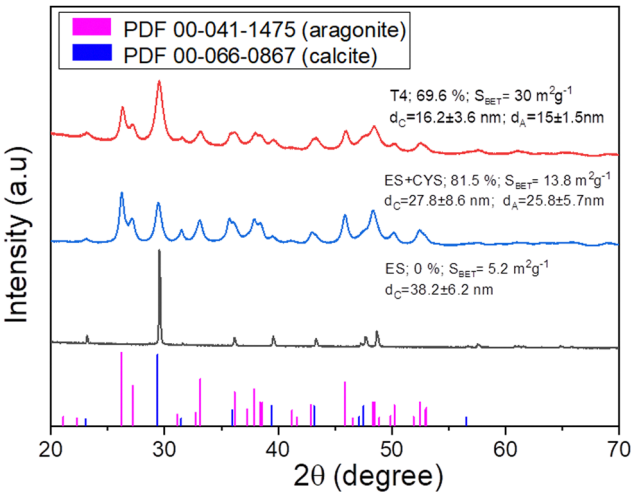


Fig. 4 X-ray diffraction patterns of the ES + ESM. ES and ES with 5% of L-cysteine after MA in T4 conditions. The percentage content of aragonite and the estimated calcite and aragonite crystallite sizes calculated by using Le Bail refinement and the specific surface area ($S_{BET}$) values for each sample are presented in the figure.

To confirm the important role of the ESM in the transformation, the mechanical activation of the eggshell without the outer and inner membrane (ES) was carried out under T4 conditions. These conditions were selected, as a high amount of aragonite after a relatively short time (1 hour) of treatment was obtained. Although there are other samples with comparable aragonite content (such as T8, T10, T12 and T16), two and more hours of milling, respectively, are necessary to reach the similar phase composition.

Fig. 4 shows the XRD patterns of ES treated under T4 conditions. Clearly, only pure calcite phase (PDF 00-066-0867) was found upon milling ES where ESM was removed, which confirms the valuable role of ESM in the transformation (see Fig. 4). In order to see whether the organic material needs to be naturally embedded (like in the case of natural ESM) or can be also artificially supplied to make the transformation to occur, an additional experiment with the 5% artificially added organic matter to the ESM-free eggshell was performed. L-cysteine amino acid (CYS) was selected due to the similarity to ESM in the presence of sulphur (ESM also contains around 3% of it). In the XRD pattern of this mixture treated under T4 conditions, a mixture of calcite and aragonite (PDF 00-041-1475) phases can be seen, which confirmed the successful calcite-to-aragonite transformation also in this case.

 

The estimated aragonite content in the ES + CYS was higher than in the ES + ESM sample treated under T4 conditions. The difference in the degree of phase transformation may be due to the higher content of organic material in the ES + CYS sample (we have introduced 5% of the organic material, whereas the organic ESM represents around 3.5% of the ES weight). Also in ES + CYS, a significantly larger amount of sulphur was introduced (its content is around 3% sulfur and more than 26% for ESM and cysteine, respectively). The estimated crystallite size of both phases is around 25 nm, which is similar to that of aragonite reported in ref. 13. Calcite crystallite size was lower (between 10 and 15 nm) in the mentioned study.

The specific surface area values of both ES and ES + CYS samples are significantly lower in comparison with that of ES + ESM (all the samples were treated under T4 conditions). The difference in the surface area can be explained by the way organic substances interact with ES. In the case of ES + ESM, organics are contained in the form of an outer membrane (film) and an inner membrane, which were strongly embedded and interconnected with the ES.[24] And during milling, the decomposition of organic matter in the structure slows down the agglomeration process. In the case of ES with CYS, they are simply a mechanical mixture, which, during milling agglomerates and reduces the specific surface area. $S_{BET}$ changes are definitely not related to the amount of aragonite present, as noted in the previous work.[13]

The influence of the mechanical activation of ES, ES + ESM and ES + CYS samples on their morphology was pursued by using scanning electron microscopy. The micrographs are presented in Fig. S7 in the ESI.†

SEM images show the presence of both large and small grains in all the samples. However, in the ES + CYS (Fig. S7c, ESI†), more finer particles are observed than upon pure ES treatment. For the ES + ESM sample, the number of finer particles is even higher. Fine particles in the ES + ESM and ES + CYS samples are numerous, and their presence is most probably the reason for the higher specific surface area in comparison with pure ES. The elemental mapping has shown the homogeneous distribution of calcium, carbon, and oxygen in all three samples (Fig. S8–S10 in the ESI†). In the case of ES + CYS and ES + ESM samples, also a significant amount (0.89 at% and 0.74%. respectively) of sulfur was detected (see Table S3, ESI†). The reason for this is the presence of sulfur in the L-cysteine structure and in the ESM, as reported in ref. 36 and 37.

The phase transformation of calcite ($R\bar{3}c$) to aragonite ($Pmcn$) is of a reconstructive nature, and the main factor is the self-diffusion of calcium and oxygen.[38] In the process of transformation, the initial secondary structure of calcite is destroyed. At low temperatures, diffusion slows down and the secondary structure of the aragonite phase forms slowly. The presence of impurities can increase diffusion and speed up the transformation process.[39–43] It has been reported[39] that impurities can strongly inhibit the direct precipitation of calcite as well as the conversion of aragonite to calcite. The discrepancy in activation rates and energies depends on the nature of the impurity, which may be associated with the nature of grain boundaries and deformational strain.[40]

The results have shown us that the presence of organic material, either or natural origin (ESM), or artificially introduced (CYS), is crucial for the phase transformation in eggshell to occur. The positive effect of the presence of organics can be attributed to the same hypothesis[34,35] with impurities that promote the phase transition. However, as higher temperatures occur during milling, the organic material can also decompose. According to the literature,[44] sulfur-containing amino acids decompose at high temperatures with the release of carbon dioxide and hydrogen sulfide, the characteristic odor of which is observed when the chamber is opened after grinding. However, as the sulfur content was enriched during milling (the content of sulfur determined *via* EDX is higher than before, see Table S3 in the ESI†), it means that the formation of $H_2S$ is just partial, and that the $CO_2$ formation is more pronounced.

In conclusion, when generalizing the results of our experiments. we can obtain a certain pattern showing that the degree of transformation of calcite into aragonite is governed by the content of organics. In the absence of organic substances in the ES, the transformation does not occur, which was presented above. The presence of an outer membrane allowed the transformation of calcite to aragonite to reach 58%,[13] and milling of ES containing both outer and inner membrane resulted in the formation of 73.7% aragonite. Finally, treating ES with the artificially added 5 wt% of L-cysteine allowed the degree of transformation to reach 81.5% under the given conditions.

### 3.5. Phase transformation of $CaCO_3$ in commercial calcite

To investigate whether the phase transformation of calcite to aragonite can be triggered in the presence of CYS only in

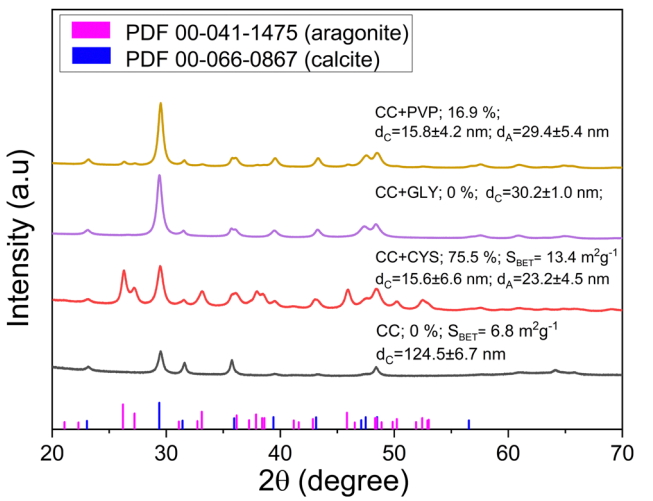


Fig. 5 X-ray diffraction patterns of the commercial calcite (CC) and a mixture of commercial calcite with 5% of L-cysteine (CYS), glycine (GLY) and polyvinyl pyrrolidone (PVP) milled under T4 conditions. The percentage content of aragonite and the estimated calcite and aragonite crystallite sizes calculated by using Le Bail refinement for each sample are presented in the figure. For CC and CC + CYS samples, also the specific surface area ($S_{BET}$) values are provided.

natural materials or also in synthetic ones, an experiment was conducted with commercial calcite (CC). For comparison, also pure CC was milled again under similar conditions. The XRD patterns, together with aragonite content and $S_{BET}$ values are shown in Fig. 5. All experiments were carried out under T4 conditions.

The phase transformation was not observed after the mechanical activation of pure commercial calcite. However, after milling CC with CYS, a mixture of calcite and aragonite phases can be seen. The content of aragonite was similar to ES + ESM and ES + CYS samples. The similarity was also discovered in the $S_{BET}$ values, as a significant increase to almost the same value as in the case of ES + CYS sample, was evidenced. The experiments with CC have shown a large similarity to the results obtained for milling of the ES with L-cysteine, or the ES + ESM sample. The effect of organic matter on aragonite formation can be compared with the formation of travertine deposits, which always contain a small amount of intruded organic matter.[37,38] Thus, the artificial introduction of organic compound can trigger the calcite–aragonite transformation also in the commercial powder.

SEM images (Fig. S11 in the ESI†) show the presence of both large and small grains. The number of fine particles in CC + CYS sample is larger than during the treatment of pure CC, similarly to to ES + CYS sample. The elemental mapping (Fig. S12 and S13 in the ESI†) has shown the homogeneous distribution of calcium, carbon and oxygen in both samples. In the CC + CYS sample, a small amount of sulfur was found, its content being below 1 wt%.

To investigate the potential universality of the calcite–aragonite phase transformation induced by the decomposition of artificially introduced organics and the role of the presence of sulfur, two other organic compounds (5 wt%) were used for the co-milling with commercial calcite instead of cysteine, namely glycine and polyvinyl pyrrolidone. The former was selected due to the fact that it is an amino acid similarly to cysteine, albeit free from sulfur, and the latter one because it is not a structural component of proteins (unlike amino acids) and it is also sulfur-free. The reaction mixtures were treated under T4 conditions and the XRD patterns are given in Fig. 5. The phase transformation in the presence of PVP proceeded to 17%, whereas in the presence of GLY, it did not occur at all. However, in the latter case, the calcite peaks are slightly shifted, meaning a change in the lattice parameters, which was observed also in ref. 45. These experiments underscore the crucial role of sulfur presence in the phase transformation. The degree of transformation might be also related to the thermal decomposition temperatures of the used organic compounds. Namely, it is equal to 221, 220 and 250 °C for CYS, PVP and GLY, respectively.[46,47] In the first two cases, the transformation was observed, whereas in the most stable organics out of the three, it did not occur. It also might be related to the total carbon content (available for decomposition/burning), since this is the highest in the case of PVP (65 wt%), followed by GLY (32 wt%) and CYS, where the transformation was the most pronounced contains 30 wt% carbon. If CYS containing sulfur is neglected, the higher C content in PVP than in GLY might result in more pronounced decomposition in the former case. The estimated crystallite size of calcite is about two times smaller in the systems where the phase transformation was observed (CC + CYS and CC + PVP) in comparison with transformation-free system (CC + GLY). It hints at the fact that the formation of aragonite crystals takes place *via* re-crystallization of part of calcite crystals. Interestingly, even in the CC + GLY system, calcite crystals are four times smaller than in pure CC, pointing to the fact that GLY is not just an inert additive, but interacts with calcite crystals, and may be serving the role of a capping agent hampering the agglomeration process. The crystallite size of aragonite in both CC + CYS and CC + PVP systems is quite similar (around 25 nm). We are aware that we only scratched the ground of the exact processes that govern this phase transformation in this study but we believe that our preliminary data could be a good basis for future research in this direction.

## 4. Conclusions

The aim of the present study was to investigate whether the presence of the organic material is mandatory for the calcite-to-aragonite phase transformation in eggshell to occur and whether the organic material can also be introduced artificially. For both these questions, this research has provided us with a positive answer. However, there seem to be limitations regarding the type of the artificially introduced organics, namely the presence of sulphur seems to be mandatory. The same is valid also for the commercial calcite powder. The degree of transformation depends on the content of organic substances in the initial material and on the energy input. However, the complete phase transformation could not be reached and if the milling is performed for too long, a backward transformation occurs. Most probably, the aragonite structure collapses once the higher pressure being created as a result of the organics decomposition is gone.

Another aim was to statistically assess the role of individual milling parameters on the degree of phase transformation in eggshell. Namely, the Taguchi method ($4^4$ orthogonal array) was used to evaluate the influence of individual milling conditions showing that sample mass is the most important for the degree of transformation. This is most probably related to the content of the organic material, namely when it is higher, it boosts the phase transformation to a larger extent.

## Author contributions

Conceptualization: M. B. Funding acquisition: M. B., B. S., F. E. Investigation: K. K., M. B., S. K., I. O. T. Project administration: M. B. Resources: M. B., F. E. Supervision: M. B. Validation: K. K., M. B. Visualization: K. K., R. D. Writing – original draft: K.K., M.B. Writing – review & editing: K. K., M. B., S. K.

 

## Data availability

The data supporting this article have been included as part of the ESI.†

## Conflicts of interest

The authors declare no conflict of interest.

## Acknowledgements

This study was funded through a grant from the Science Committee of the Ministry of Science and Higher Education of the Republic of Kazakhstan (Grant No. AP13067724). K. K. acknowledges the support of SAIA. No. within the National Scholarship Program of the Slovak Republic (scholarship ID 38734). The support of Slovak Research and Development Agency under the contract No. APVV-23-0372 and Slovak Grant Agency VEGA (project 2/0112/22) is also acknowledged. We are grateful to Dr Ummen Sabu from Clemson University, USA for sharing the procedure of separating the eggshell membrane from the eggshell.

## References

1 V. P. Balema, V. K. Pecharsky and K. W. Dennis, *J. Alloys Compd.*, 2000, **313**, 69–74.
2 X. Pan and X. Ma, *J. Solid State Chem.*, 2004, **177**, 4098–4103.
3 Y. Wang, C. Suryanarayana and L. An, *J. Am. Ceram. Soc.*, 2005, **88**, 780–783.
4 M. Baláž, in *Environmental Mechanochemistry: Recycling Waste into Materials using High-Energy Ball Milling*, ed. M. Baláž, Springer International Publishing, Cham, 2021, pp. 1–52.
5 P. Baláž, A. Calka, A. Zorkovská and M. Baláž, *Mater. Manuf. Process.*, 2013, **28**, 343–347.
6 F. Dachille and R. Roy, *Nature*, 1960, **186**, 34.
7 S. R. Chauruka, A. Hassanpour, R. Brydson, K. J. Roberts, M. Ghadiri and H. Stitt, *Chem. Eng. Sci.*, 2015, **134**, 774–783.
8 P. Xiaoyan, C. Yi, M. Xueming and Z. Lihui, *J. Am. Ceram. Soc.*, 2004, **87**, 1164–1166.
9 T. P. Shakhtshneider, *Solid State Ionics*, 1997, **101–103**, 851–856.
10 P. A. Zielinski, *J. Mater. Res.*, 1993, **8**, 2985–2992.
11 J. Y. Huang, Y. K. Wu and H. Q. Ye, *Appl. Phys. Lett.*, 1995, **66**, 308–310.
12 M. Baláž, J. Ficeriová and J. Briančin, *Chemosphere*, 2016, **146**, 458–471.
13 M. Baláž, A. Zorkovská, M. Fabián, V. Girman and J. Briančin, *Adv. Powder Technol.*, 2015, **26**, 1597–1608.
14 N. Koga, D. Kasahara and T. Kimura, *Cryst. Growth Des.*, 2013, **13**, 2238–2246.
15 F. C. Meldrum and H. Cölfen, *Chem. Rev.*, 2008, **108**, 4332–4432.
16 P. Gillet, Y. Gérard and C. Willaime, *Bull. Mineral.*, 1987, **110**, 481–496.
17 R. B. Gammage and D. R. Glasson, *J. Colloid Interface Sci.*, 1976, **55**, 396–401.
18 J. Perić, R. Krstulović, T. Ferić and M. Vučak, *Thermochim. Acta*, 1992, **207**, 245–254.
19 S. Ono, T. Kikegawa, Y. Ohishi and J. Tsuchiya, *Am. Mineral.*, 2005, **90**, 667–671.
20 T. Li, F. Sui, F. Li, Y. Cai and Z. Jin, *Powder Technol.*, 2014, **254**, 338–343.
21 G. Martinez, J. Morales and G. Munuera, *J. Colloid Interface Sci.*, 1981, **81**, 500–510.
22 D. O. Northwood and D. Lewis, *Canadian Mineral.*, 1970, **10**, 216–224.
23 M. Baláž, *Adv. Colloid Interface Sci.*, 2018, **256**, 256–275.
24 J. Gautron, L. Stapane, N. Le Roy, Y. Nys, A. B. Rodriguez-Navarro and M. T. Hincke, *BMC Mol. Cell Biol.*, 2021, **22**, 11.
25 A. B. Rodríguez-Navarro, P. Marie, Y. Nys, M. T. Hincke and J. Gautron, *J. Struct. Biol.*, 2015, **190**, 291–303.
26 M. Baláž, *Acta Biomater.*, 2014, **10**, 3827–3843.
27 A. Zorkovská and P. Baláž, *Mater. Struct.*, 2011, **18**, 188–190.
28 F. Garcia, N. Le Bolay and C. Frances, *Chem. Eng. J.*, 2002, **85**, 177–187.
29 R. Davis, P. John, R. Davis and P. John, *Statistical Approaches With Emphasis on Design of Experiments Applied to Chemical Processes*, IntechOpen, 2018.
30 G. Taguchi, R. Jugulum and S. Taguchi, *Computer-based Robust Engineering: Essentials for DFSS*, ASQ Quality Press, 2004.
31 B. H. Toby and R. B. Von Dreele, *J. Appl. Crystallogr.*, 2013, **46**, 544–549.
32 H. Pesenti, M. Leoni and P. Scardi, *Z. Kristallogr. Suppl.*, 2008, 143–150.
33 M. Radune, S. Lugovskoy, Y. Knop and A. Yankelevitch, *Int. J. Mech. Mater. Eng.*, 2022, **17**, 1.
34 A. A. L. Michalchuk and F. Emmerling, *Angew. Chem., Int. Ed.*, 2022, **61**, e202117270.
35 I. Halasz, S. A. J. Kimber, P. J. Beldon, A. M. Belenguer, F. Adams, V. Honkimäki, R. C. Nightingale, R. E. Dinnebier and T. Friščić, *Nat. Protoc.*, 2013, **8**, 1718–1729.
36 V. K. Kodali, S. A. Gannon, S. Paramasivam, S. Raje, T. Polenova and C. Thorpe, *PLoS One*, 2011, **6**, e18187.
37 N. Li, L. Niu, Y. Qi, C. K. Y. Yiu, H. Ryou, D. D. Arola, J. Chen, D. H. Pashley and F. R. Tay, *Biomaterials*, 2011, **32**, 8743–8752.
38 N. S. Bagdassarov and A. B. Slutskii, *Phase Transit.*, 2003, **76**, 1015–1028.
39 M. S. Hashim and S. E. Kaczmarek, *Earth Planet. Sci. Lett.*, 2021, **574**, 117166.
40 S.-J. Lin and W.-L. Huang, *Contrib. Mineral. Petrol.*, 2004, **147**, 604–614.
41 T. Isobe and M. Senna, *J. Chem. Soc., Faraday Trans. 1*, 1988, 1199–1209.
42 Y.-P. Lin and P. C. Singer, *Water Res.*, 2005, **39**, 4835–4843.
43 Q. L. Feng, G. Pu, Y. Pei, F. Z. Cui, H. D. Li and T. N. Kim, *J. Cryst. Growth*, 2000, **216**, 459–465.
44 I. M. Weiss, C. Muth, R. Drumm and H. O. K. Kirchner, *BMC Biophys.*, 2018, **11**, 2.
45 D. Zhuang, H. Yan, Z. Han, H. Zhao and M. E. Tucker, *Carbonates Evaporites*, 2020, **35**, 44.
46 I. M. Weiss, C. Muth, R. Drumm and H. O. K. Kirchner, *BMC Biophys.*, 2018, **11**, 2.
47 V. M. Bogatyrev, N. V. Borisenko and V. A. Pokrovskii, *Russ. J. Appl. Chem.*, 2001, **74**, 839–844.